The Canadian Mineralogist
Vol. 43, pp. 35-50 (2005)

ESTIMATING P-T CONDITIONS OF GARNET GROWTH WITH ISOCHEMICAL PHASE-DIAGRAM SECTIONS AND THE PROBLEM OF EFFECTIVE BULK-COMPOSITION

DOUGLAS K. TINKHAM[§] AND EDWARD D. GHENT

Department of Geology and Geophysics, University of Calgary, Calgary, Alberta T2N 1N4, Canada

ABSTRACT

Isochemical pressure–temperature phase-diagram sections portray the theoretical equilibrium distribution of mineral assemblages and mineral compositions for a given bulk-composition. To utilize such isochemical sections to derive the P–T conditions of garnet growth requires knowledge of the effective bulk-composition, defined as the rock composition available to the reacting assemblage of phases. Isochemical sections for a Canadian Cordillera garnet – muscovite – biotite – kyanite – plagioclase – quartz – rutile – ilmenite – graphite pelite from the kyanite zone at Mica Dam, British Columbia, were calculated in the system $MnO–Na_2O–CaO–K_2O–FeO–MgO–Al_2O_3–SiO_2–H_2O–TiO_2$ using bulk compositions derived by X-ray-fluorescence (XRF) analysis and quantitative X-ray mapping with an electron-probe micro-analyzer (EPMA). Isopleths of measured compositions of the core of the garnet are plotted on isochemical sections to estimate P–T conditions of core growth. Comparison of measured compositions of the core with those predicted from the phase-diagram sections for the XRF-derived composition indicates that initial growth of garnet in this sample occurred at approximately 7.7 kilobars and 555°C, and multi-equilibrium garnet-rim thermobarometry yields 7.2 kilobars, 680°C. Therefore, there is no discernable difference in pressure of formation between core and rim. Recent literature suggests that XRF-derived compositions are not suitable for estimating effective bulk-compositions, but we stress that they may be appropriate in certain situations. Coarse-grained samples require X-ray mapping over prohibitively large areas to obtain effective bulk-compositions. In this study, we dealt with a medium- to coarse-grained pelite. XRF-derived compositions are likely to be suitable in this situation. The benefits of EPMA compositions include the ability to exclude specific phases from the composition, or even exclude portions of compositionally zoned phases to model the evolution of the effective bulk-composition during growth of zoned phases. Garnet is the only phase in this sample that exhibits significant chemical zonation. Quantitative X-ray maps were used to calculate an integrated composition of garnet that was subsequently subtracted from the XRF-derived bulk-composition to model the effect of bulk-rock fractionation during garnet growth. An isochemical section calculated with this fractionated composition predicts that garnet will react into the assemblage at P–T conditions similar to that calculated by garnet-rim thermobarometry, suggesting that the method used to model fractionation is appropriate.

Keywords: phase equilibria, bulk composition, garnet, isochemical section, phase diagram, Mica Creek, British Columbia.

SOMMAIRE

Nous utilisons des sections de pression–température isochimiques d'un diagramme de phases approprié pour obtenir la distribution à l'équilibre des assemblages de minéraux et leur composition pour une composition globale donnée. L'utilisation de telles sections isochimiques pour dériver les conditions P–T de croissance du grenat requiert une composition globale effective, que nous définissons comme la composition de la roche disponible à l'assemblage de phases lors de la réaction. Nous avons calculé de telles sections isochimiques pour une pélite contenant l'assemblage grenat – muscovite – biotite – kyanite – plagioclase – quartz – rutile – ilménite – graphite provenant de la zone à kyanite à Mica Dam, en Colombie-Britannique, Cordillères canadiennes, en termes du système $MnO–Na_2O–CaO–K_2O–FeO–MgO–Al_2O_3–SiO_2–H_2O–TiO_2$ en utilisant des compositions globales dérivées par fluorescence X (XRF) et par répartition quantitative des éléments par cartographie des rayons X avec une microsonde électronique (EPMA). Les isoplèthes de compositions mesurées du coeur du grenat sont posées sur les sections isochimiques pour évaluer les conditions P–T de croissance du coeur. Une comparaison des compositions mesurées du coeur des cristaux avec celles qui sont prédites à partir des sections construites avec la composition globale XRF indique un début de croissance à environ 7.7 kilobars et 555°C, et une approche par thermobarométrie multi-équilibre utilisant la bordure des grains de grenat mène à 7.2 kilobars, 680°C. Il n'y a donc aucune différence discernable en pression entre le coeur et la bordure des grains de grenat. D'après la littérature récente, les compositions dérivées par fluorescence X ne seraient pas appropriées pour estimer la composition globale effective, mais nous croyons qu'elles peuvent l'être dans certaines situations. L'alternative pour des échantillons à grains grossiers serait de cartographier avec rayons X des superficies beaucoup trop grandes. Dans ce travail, les sections isochimiques sont utilisées pour délimiter les conditions P–T de croissance du coeur de grenat dans une pélite à grains moyens à grossiers. Les

§ *E-mail address*: tinkham@ucalgary.ca

compositions dérivées d'une analyse XRF sont plus aptes à être appropriées dans ce cas. Parmi les bénéfices des compositions globales calculées à partie d'analyses ponctuelles des minéraux, il y a l'abilité d'exclure certaines phases de la composition globale calculée, ou bien des portions zonées de phases, afin d'évaluer l'évolution de la composition globale effective pendant la croissance des phases zonées. Seul le grenat montre une zonation importante dans cet échantillon. Des cartes quantitatives de répartition des rayons X ont été utilisées pour calculer la composition intégrée du grenat, laquelle a ensuite été soustraite de la composition XRF afin d'évaluer le fractionnement de la roche globale au cours de la croissance du grenat. Une section isochimique calculée avec cette composition fractionnée prédit que le grenat paraitra dans cet assemblage à des conditions P–T semblables à celles préconisées par thermobarométrie effectuée avec la bordure du grenat, ce qui fait penser que la méthode utilisée pour simuler le fractionnement est appropriée.

(Traduit par la Rédaction)

Mots-clés: équilibre de phases, composition globale, grenat, section isochimique, diagramme de phases, Mica Creek, Colombie-Britannique.

Introduction

Understanding the processes that occur in cores of orogenic belts requires knowledge of the changes in pressure and temperature that a rock experiences during orogeny. Documenting such changes in pressure and temperature is possible by combining an understanding of the P–T stability field of observed assemblages of minerals with the application of thermobarometric methods to coexisting phases presumed to have been in equilibrium during some portion of the metamorphic recrystallization history. However, the determination of changes in pressure and temperature during metamorphism in a quantitative manner is a daunting task (Ghent *et al.* 1989). The process usually involves interpretation of reaction textures and an inference concerning the changes in pressure and temperature needed to produce such reaction textures. This approach reduces the estimated change in pressure and temperature to a qualitative determination only. Furthermore, the use of reaction textures to infer P–T paths should be done with extreme care, as different P–T paths can lead to the same observed texture, and hence could result in inaccurate conclusions regarding the nature of the P–T path (see Kelsey *et al*. 2003). Direct quantitative calculation of garnet-growth P–T paths using inclusion-suite thermobarometry (St-Onge 1987) and the Gibbs Method (Spear & Selverstone 1983) is possible, but samples suitable for application of these techniques are quite rare in our experience.

An alternative method for constraining P–T paths of garnet growth was outlined by Vance & Mahar (1998). They utilized isochemical sections and compositions of garnet crystal cores to constrain the P–T conditions of growth of the garnet cores. [The phrase isochemical sections used here is shorthand for isochemical P–T phase-diagram sections. These types of diagrams have traditionally been called pseudosections. The term *pseudosection* implies "false section". However, these diagrams are true sections through the phase diagram at constant chemical composition, and we therefore prefer not to use the term *pseudosection* in this context.] This technique has yielded geologically sensible results in several studies (*e.g.*, Stowell & Tinkham 2003, Tinkham 2002). The technique involves measuring the composition of the initial growth core (chemical core) of garnet, casting that composition in terms of the compositional variables used in constructing the phase-diagram section, and plotting the corresponding compositional isopleths on the section. The P–T point where all the isopleths come the closest to intersecting is taken as the best estimate of the P–T conditions of growth of the core. In practice, the uncertainty in the P–T location of each isopleth is plotted, and the region where the uncertainties all overlap is taken as the P–T estimate.

In this paper, we constrain the P–T conditions of garnet growth in a metapelite from the Mica Creek area of British Columbia by combining isochemical P–T phase diagram sections and techniques of multi-equilibrium thermobarometry (Powell & Holland 1994). The P–T conditions of growth of a garnet core were estimated using a phase-diagram section constructed for a bulk-rock composition obtained from results of an XRF analysis of the rock. A second phase-diagram section was constructed to calculate the P–T stability of the observed (peak) assemblage from the same sample, and to illustrate the effect of growth-induced fractionation on assemblage stability. The rock composition used in the construction of this section was obtained by removing an integrated composition of the garnet, calculated from quantitative X-ray maps, from the XRF-derived bulk-rock composition. The phase equilibria of pelitic rocks in the MnNCKFMASHT system ($MnO–Na_2O–CaO–K_2O–FeO–MgO–Al_2O_3–SiO_2–H_2O–TiO_2$) are illustrated with these isochemical sections, and problems associated with the method of determining effective bulk-composition are discussed.

Geological Setting

The Mica Creek area has been the subject of several papers on the petrology, structure, stratigraphy, stable isotope geochemistry, geochronology, and geothermobarometry of the metamorphic rocks. For references, see Crowley *et al*. (2000), Ghent & Gordon (2000), Ghent & Valley (1998), and Digel *et al.* (1998). The area is

underlain by pelite, semipelite, amphibolite and marble of the Late Precambrian Mica Creek assemblage, the lower division of the Horsethief Creek Group (Raeside & Simony 1983). The metamorphic grade ranges from the upper garnet zone to K-feldspar – quartz – sillimanite zone in metapelites (Fig. 1). The coexistence of staurolite + kyanite, the presence of a broad staurolite-absent kyanite zone, and the occurrence of clinopyroxene + garnet + quartz metabasic rocks in upper amphibolite facies units suggest pressures higher than those typical of Barrovian metamorphism (*e.g,* Spear 1993).

Petrography and Mineral Compositions

Rock and mineral descriptions

Sample MC–01–97 is a medium- to coarse-grained Grt – Ms – Bt – Ky – Pl – Qtz schist with minor apatite, rutile, graphite, and rare ilmenite and titanite (phase abbreviations follow those of Kretz 1983). Quartz + plagioclase leucosomes up to 1 cm in width are locally present. Schistosity is defined by the alignment of biotite and muscovite. Both muscovite and biotite are locally oblique to the predominant schistosity. Anhedral to euhedral porphyroblasts of garnet range from 1.5 to 8 mm in diameter, and the schistosity is typically deflected around the larger porphyroblasts. The garnet contains abundant inclusions of quartz, minor biotite, muscovite, and rutile, and rare inclusions of titanite and apatite. The pattern of inclusions locally appears to define an internal foliation oblique to matrix schistosity. Kyanite porphyroblasts are elongate and are very weakly aligned within the schistosity.

Rutile predominantly occurs as inclusions within garnet, and rare ilmenite is present in the matrix. Apatite predominantly occurs as a matrix phase, but very rare apatite occurs as inclusions within garnet.

Mineral compositions

Electron-probe micro-analysis studies were performed on the JEOL–8200 instrument at the University

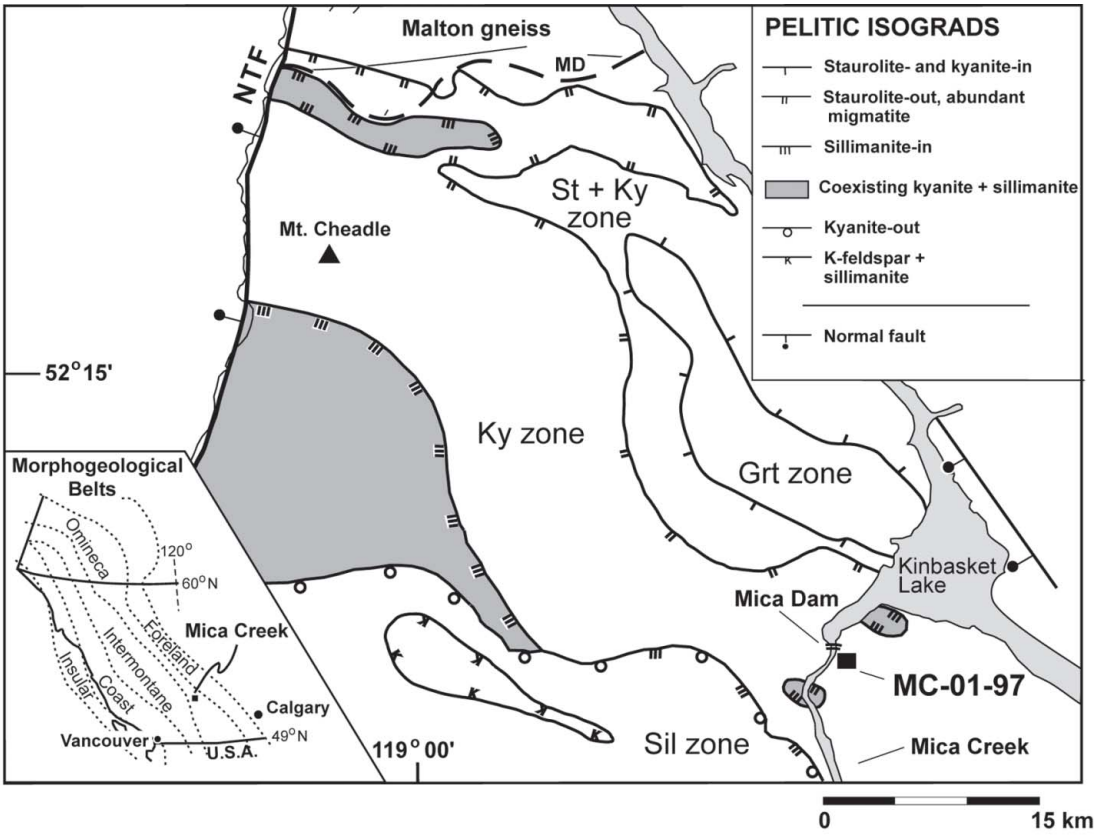

FIG. 1. Isograd map of the Mica Creek region, British Columbia, showing location of sample MC–01–97 in the kyanite zone adjacent to Mica Dam. NTF: North Thompson Fault, MD: Malton Detachment. Modified from Digel *et al.* (1998).

of Calgary. Operating conditions were 15 kV accelerating voltage, 15–20 nA beam current, 1–10 μm beam diameter, and peak-count times of 20–30 seconds. For corrections to the X-ray count data, we utilized a ZAF algorithm provided with the JEOL software. Quantitative X-ray maps were collected at an accelerating voltage of 15 kV , a beam current of 80 nA , a beam diameter of 2 μm, and peak-count times of 180 ms per pixel. X-ray maps were processed with the program XRMapAnal (Tinkham & Ghent, in press) to calculate mineral modes and compositions from the maps.

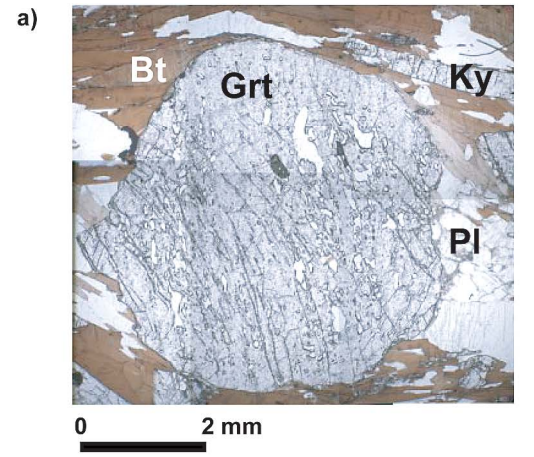

FIG. 2. Garnet from sample MC–01–97. (a) Photomicrograph of garnet porphyroblast. (b) Mn*K*α X-ray map. A–A' shows position of garnet linescan in Figure 3.

Garnet crystals with a diameter less than approximately 3 mm are typically homogeneous in the interior, with Mn enrichment along the edge. Larger crystals are chemically zoned (Figs. 2, 3), with a spessartine component decreasing from core to rim, and pyrope and almandine content increasing from core to rim. Zoning in the grossular component is weak, with a slight decrease from core to rim. Garnet zoning is interpreted to result from primary growth. Most crystals show a slight increase in the spessartine component and decrease in the pyrope component at their margin, which is interpreted to represent late-stage diffusional modification of the growth zoning and possibly minor resorption.

Muscovite and biotite lack chemical zoning. Representative compositions are given in Table 1. Plagioclase is relatively homogeneous, but locally exhibits a minor (up to 2%) increase in the albite component and decrease in the anorthite component at the rim of crystals (Fig. 4). An average composition of the plagioclase is given in Table 1.

BULK-ROCK COMPOSITIONS

Isochemical sections can be used to constrain the P–T conditions of metamorphism and P–T trajectories by

TABLE 1. MINERAL COMPOSITIONS DERIVED FROM ELECTRON-PROBE MICRO-ANALYTICAL DATA FOR SAMPLE MC–01–97

	Bt *n* = 13	Ms *n* = 13	Pl *n* = 106	Grt rim *n* = 14	Grt core *n* = 5
SiO_2 wt.%	35.81	46.31	62.95	37.70	37.91
Al_2O_3	20.32	35.89	23.50	21.24	21.04
TiO_2	2.21	0.68	n.a.	0.01	0.00
FeO	18.06	1.15	0.03	35.34	33.37
MgO	9.52	0.81	n.a.	3.95	3.59
MnO	0.07	0.01	n.a.	1.95	3.75
CaO	0.00	0.00	3.95	1.23	1.88
Na_2O	0.38	0.90	9.34	n.a.	n.a.
K_2O	8.62	9.49	0.12	n.a.	n.a.
BaO	0.15	0.21	0.02	n.a.	n.a.
Cl	0.00	0.01	n.a.	n.a.	n.a.
F	0.11	0.04	n.a.	n.a.	n.a.
Total	95.25	95.50	99.90	101.40	101.54
Si *apfu*	2.695	3.064	2.785	2.989	3.003
Al	1.803	2.798	1.225	1.984	1.965
Ti	0.125	0.034	-	0.000	0.000
Fe	1.137	0.064	0.001	2.343	2.211
Mg	1.068	0.079	-	0.466	0.424
Mn	0.004	0.000	-	0.131	0.251
Ca	0.000	0.000	0.187	0.104	0.159
Na	0.055	0.115	0.801	-	-
K	0.828	0.801	0.007	-	-
Ba	0.004	0.005	0.000	-	-
Cl	0.001	0.001	-	-	-
F	0.026	0.009	-	-	-

End-member proportions

phl	0.075	ms	0.714	ab	0.805	alm	0.770	0.726
ann	0.429	pg	0.115	an	0.188	prp	0.153	0.139
east	0.497	ma	0.000	ksp	0.007	grs	0.034	0.052
mnbi	0.001	cel	-0.059			sps	0.043	0.083
obi	-0.127	fcel	0.073					
tibi	0.125	prl	0.083					

n.a.: not analyzed; *n*: number of analyses made. The number of atoms was calculated on the basis of 22 negative charges for biotite and muscovite, 16 for plagioclase, and 24 for garnet.

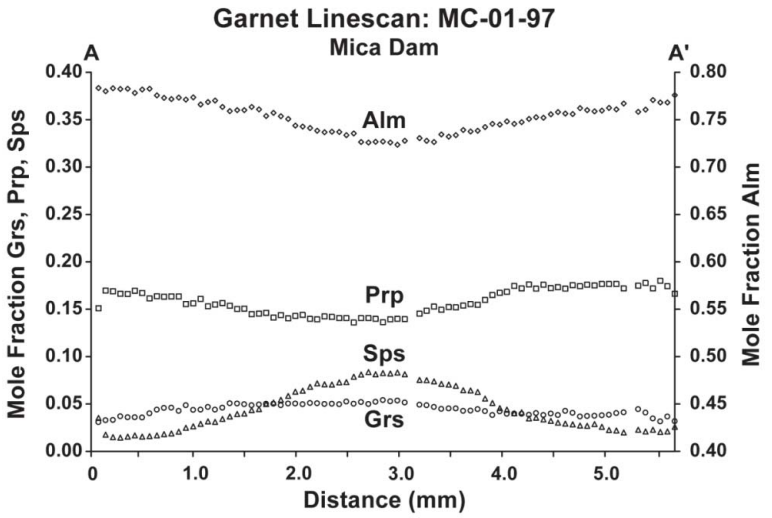

FIG. 3. Electron-probe micro-analyzer linescan across garnet shown in Figure 2. Symbols of components: Alm: almandine, Prp: pyrope, Grs: grossular, Sps: spessartine.

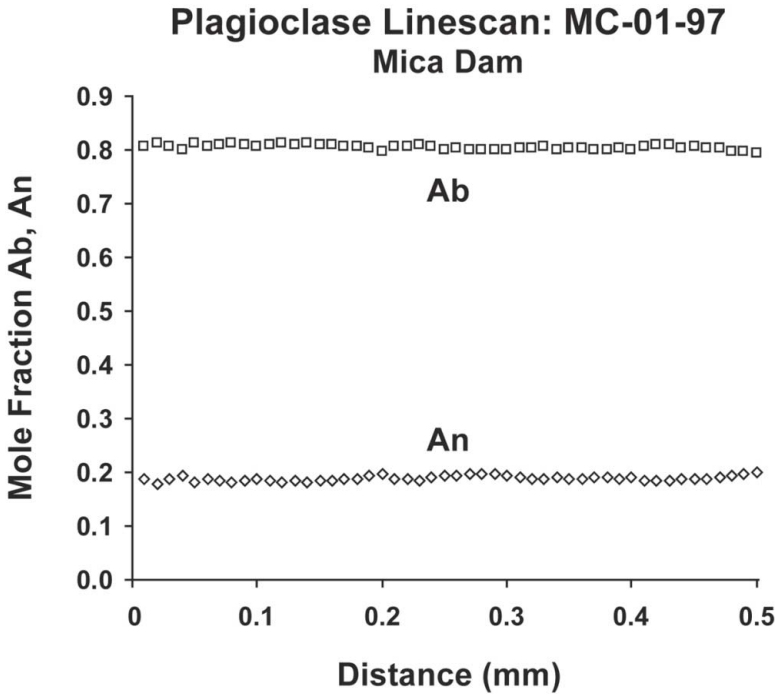

FIG. 4. Electron-probe micro-analyzer linescan across plagioclase. Note the very minor zoning at the right margin of the profile. Ab: albite component, An: anorthite component.

comparing measured compositions of phases, modes, and observed textures due to a reaction with those predicted by the section. A prerequisite for successful application of this technique is knowledge of the effective bulk-composition (see Stüwe 1997), defined here as that composition available to the reacting assemblage of minerals at the time the measured compositions and modes of phases developed, or the time the observed reaction-induced textures developed. It is not expected that the effective bulk-composition for many samples remained constant throughout the history of metamorphic recrystallization. Some phases, particularly garnet in pelites, are typically chemically zoned from core to rim, indicating that the composition available to the reacting assemblage of phases changed during growth of the zoned phase. The effective bulk-composition at the time of initial equilibration and final equilibration of garnet growth is of particular interest in this study.

There are several methods available for estimating the effective bulk-composition during the initial stages of garnet growth. One method utilizes the result of a bulk-rock X-ray-fluorescence analysis as an estimate of the effective composition. Another involves integrating an estimate of the modal abundance of all phases with some average composition of the phases to obtain an overall bulk-composition. Finally, a third method involves quantitative X-ray mapping over a selected area of the sample (Marmo *et al.* 2002), with a calculation of the composition at each map pixel and integrating to obtain the effective composition. The X-ray mapping method has some advantages over the other methods, but is not always feasible, depending on the size of the area required to be mapped. Some of the advantages of quantitative X-ray maps include the ability to selectively eliminate individual phases or portions of phases that are interpreted not to have been reacting during recrystallization of surrounding phases, and the ability to eliminate compositional domains that are distinctly different from that of the region of primary interest in compositionally layered samples. If the compositional domains of interest are on the order of 1 cm wide or greater, individual domains can be separated and analyzed with X-ray fluorescence spectroscopy, and the X-ray mapping technique does not offer an advantage in terms of analyzing individual domains. Further, coarse-grained samples may require X-ray mapping over a prohibitively large area to obtain a bulk composition appropriate for the sample. We therefore stress that the best method for obtaining an effective bulk-composition is dictated by the purpose of the phase-equilibria modeling. If the goal is to constrain the P–T conditions of growth of the core of garnet crystals in relatively coarse-grained pelites, an appropriate composition is likely to be obtained from an X-ray-fluorescence analysis of a carefully selected sample. However, if the goal is to elucidate the P–T conditions of peak metamorphism and zoned phases are present, significant processing of quantitative X-ray maps collected over carefully selected areas is required.

In this study, compositions derived by X-ray fluorescence, those derived from an X-ray map, and multi-equilibria thermobarometry are utilized to constrain the P–T conditions of growth of the core and rim of garnet. The bulk-rock composition used to model growth of the garnet core was obtained from results of an X-ray-fluorescence analysis of the hand sample (Table 2) . If this composition is representative of the effective bulk-composition during the initial growth of the garnet cores, it has to be assumed that there were no phases present that exhibited significant chemical zonation at the time of initial growth of the garnet, and that the composition of the portion of rock analyzed is representative of the rock composition at the time garnet crystals initially began to grow. The portion of the sample that was analyzed using X-ray-fluorescence analysis included a representative amount of leucosome material currently observed in the hand sample, and our assumption is therefore that the quartz + plagioclase leucosomes are locally derived. We stress that this does not require that the leucosomes are the product of partial melting.

To model the effect of growth-induced fractionation by garnet, quantitative X-ray maps were used to calculate an integrated composition of garnet to subtract from the bulk-rock composition. Quantitative X-ray maps were collected at the University of Calgary on a JEOL 8200 electron-probe micro-analyzer equipped with five wavelength-dispersion spectrometers. A total of 10 maps were collected, for the elements Mn, Na, Ca, K, Fe, Mg, Al, Si, P and Ti, requiring two stages of mapping. Raw X-ray counts were converted to weight percent oxide using a Bence–Albee algorithm (Bence & Albee 1968, Clarke *et al*. 2001) and the program XRMapAnal (Tinkham & Ghent 2005). Examples of oxide-distribution maps displayed as molar proportions

TABLE 2. ROCK COMPOSITIONS FOR SAMPLE MC–01–97 USED IN THE CONSTRUCTION OF ISOCHEMICAL SECTIONS OF THE P–T PHASE DIAGRAM

	XRF-derived bulk rock	Modified bulk rock*
SiO_2 wt.%	66.02	67.95
Al_2O_3	15.05	15.11
FeO	8.68	6.55
MnO	0.12	0.02
MgO	5.47	5.41
CaO	0.63	0.52
Na_2O	1.02	1.08
K_2O	2.24	2.51
TiO_2	0.71	0.79
P_2O_5	0.06	0.07
Total	100.00	100.00
Fe/(Fe + Mg)	0.613	0.547
Mn/(Fe + Mg + Mn)	0.008	0.002

Oxides are given in molecular proportions, and are the values input into the program THERMOCALC. * The modified bulk-rock composition was calculated by removing an integrated composition of garnet obtained from quantitative X-ray mapping from the bulk-rock XRF-derived composition. The component P_2O_5 was not used for phase-diagram constructions.

were calculated with program XRMapAnal and are shown in Figure 5. Removal of garnet from the XRF-derived composition to yield the garnet-removed rock composition required an estimate of the representative mode of garnet in the sample, and an estimate of an integrated composition of the garnet. The mode of garnet was estimated from the entire thin section used for X-ray mapping and the surfaces of the rock chips crushed for the XRF analysis, resulting in an estimate of 9.8%. An integrated composition of the garnet was obtained from the quantitative X-ray maps by first removing selective portions of the garnet, taking into account the geometry of Mn zoning in the garnet, to yield a region of garnet extending from the chemical core to the rim of the garnet, shown in Figure 5f. The compositions of the remaining garnet pixels shown in Figure 5f were integrated to obtain a composition that approximates the entire integrated composition of the garnet. This composition, combined with the total mode of garnet, was subtracted from the XRF composition. The resulting composition (Table 2) was used to construct the isochemical section used to constrain P–T conditions at the garnet rim.

Isochemical Pressure–Temperature Sections of the Phase Diagram

Isochemical sections were constructed in the 10-component system $MnO–Na_2O–CaO–K_2O–FeO–MgO–Al_2O_3–SiO_2–H_2O–TiO_2$ using the program THERMOCALC (Powell & Holland 1988) and an updated version of the Holland & Powell (1998) thermodynamic dataset (th.pd datafile created Feb. 13, 2002). Activity models used in the construction of isochemical sections follow those of Tinkham *et al.* (2001), except where noted in the Appendix. A pure H_2O fluid and quartz are considered in excess in all calculations. The pure H_2O fluid used in calculations is likely only an approximation to the actual composition of fluid. The presence of graphite in the sample indicates that in reality the fluid is a C–O–H fluid, and likely buffered to a high activity of H_2O (Connolly & Cesare 1993). The activity of H_2O in a graphite-saturated C–O–H fluid at 7 kilobars and 650°C (conditions appropriate for this sample) is 0.95 (calculated with program Perple_X; Connolly & Petrini 2002). At these conditions, assemblage boundaries generally shift by less than 5–8°C. Isochemical sections were constructed in the interval 3–12 kilobars, 400–700°C to cover the P–T conditions of interest in the Mica Creek region. As discussed in Tinkham *et al.* (2001), the system $MnO–Na_2O–CaO–K_2O–FeO–MgO–Al_2O_3–SiO_2–H_2O$ is considered the minimal one required to adequately model the composition of natural garnet in typical metapelitic rocks. White *et al.* (2000) presented isochemical and T–X sections and activity models for use with the Holland & Powell (1998) thermodynamic dataset with the components TiO_2 and Fe_2O_3 added to the base chemical system $K_2O–FeO–MgO–Al_2O_3–SiO_2–H_2O$. However, without an acceptable method for determining the oxidation state of Fe in Mica Creek pelites at the time of garnet growth, we decided not to include the Fe_2O_3 component, but did include TiO_2 in an attempt to model rutile and ilmenite stability. Titanium is a common component of biotite in metapelites, and Ti was therefore introduced into the structure of biotite using the site-occupancy scheme and interaction parameters of White *et al.* (2000).

An isochemical section for the XRF-derived bulk-rock composition is shown in Figure 6a. The stability field of garnet, marked by the thick blue line in Figure 6a, indicates that the lower-temperature stability of garnet is 475°C at 12 kilobars, and 530°C at 2.25 kilobars. The lowest-pressure stability in the section is 2.25 kilobars at 530°C. Paragonite stability is predicted at lower temperatures and higher pressures, whereas plagioclase stability is predicted at higher temperatures and lower pressures. There is a zone over which neither paragonite nor plagioclase is stable, and bulk-rock Na and Ca are incorporated into muscovite ± garnet at these conditions. This situation is a result of the rock having low Na and Ca contents. Chloritoid is restricted to low temperatures and higher pressures, whereas cordierite is restricted to lower pressures and higher temperatures. Staurolite stability is predicted to extend from approximately 3 kilobars to >12 kilobars, and 515° to 650°C. Aluminum silicate is not predicted to be stable at the triple point (3.8 kilobars, 505°C). Rutile stability is restricted to pressures above 8 kilobars at temperatures above 530°C, but extends to less than 2 kilobars at temperatures below 460°C. Ilmenite stability is restricted to pressures less than 9 kilobars at temperatures above 530°C, but extends to pressures below 2 kilobars at temperatures greater than approximately 460°C.

An isochemical section for the garnet-subtracted XRF-derived bulk-composition is shown in Figure 7a. This composition was derived, as discussed above, by subtracting an integrated composition of the garnet, obtained from X-ray maps, from the bulk-rock XRF-derived composition. This section was constructed to illustrate the effect of garnet fractionation on predicted stability and composition of the garnet; therefore, only the garnet-stable portion of the section is shown. The garnet-in line for the XRF-derived composition is indicated to illustrate how far this line shifts up temperature and pressure owing to garnet fractionation.

P–T Conditions of Garnet Growth

The P–T conditions of growth of the garnet core were derived from the XRF-derived isochemical section by plotting measured compositional isopleths for the garnet core on the section (Fig. 6b). Uncertainties concerning the location of these isopleths (as calculated with the program THERMOCALC) are indicated by yellow shading. The section was constructed with the linearly independent components almandine (Alm), pyrope

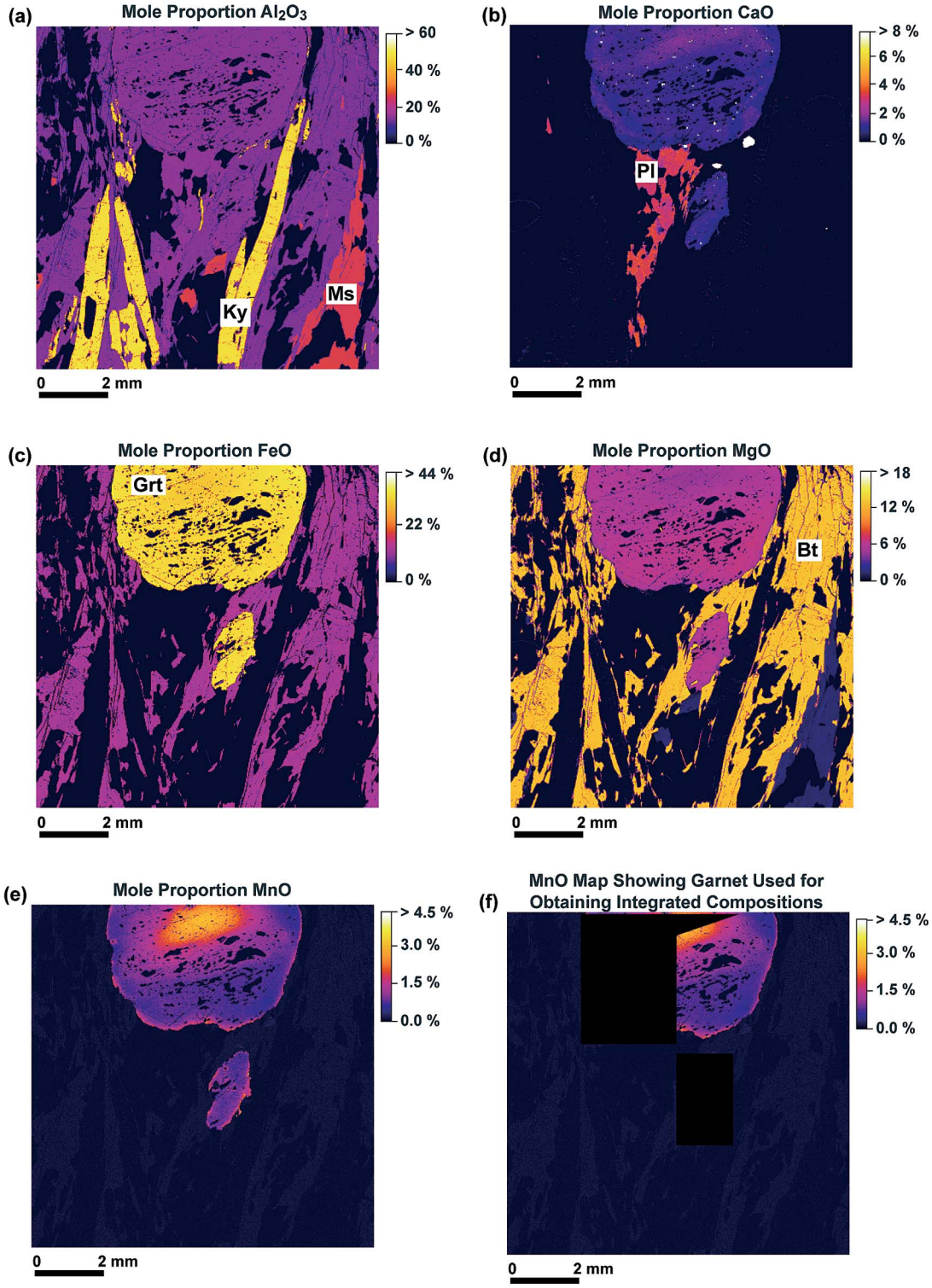
(a)
Mole Proportion Al_2O_3
> 60
40 %
20 %
0 %
Ky
Ms
0
2 mm
(b)
Mole Proportion CaO
> 8 %
6 %
4 %
2 %
0 %
Pl
0
2 mm
(c)
Mole Proportion FeO
> 44 %
22 %
0 %
Grt
0
2 mm
(d)
Mole Proportion MgO
> 18
12 %
6 %
0 %
Bt
0
2 mm
(e)
Mole Proportion MnO
> 4.5 %
3.0 %
1.5 %
0.0 %
0
2 mm
(f)
MnO Map Showing Garnet Used for Obtaining Integrated Compositions
> 4.5 %
3.0 %
1.5 %
0.0 %
0
2 mm

(Prp) and grossular (Grs). The overlap of the compositional isopleths for the garnet core (within uncertainty) for these three end-members is taken as the best approximation of core growth (7.7 kilobars, 555°C). The overlap occurs in the assemblage Grt + Ctd + Chl + Ms + Ilm + Qtz + H_2O. Both chloritoid and ilmenite are not observed as inclusions near the core. This does not represent a problem, as there is no reason to expect that every phase stable at the beginning of garnet growth will necessarily be preserved as an inclusion in it. However, there are minor inclusions of rutile within garnet, and its presence is not predicted by the phase-diagram section. It is possible that the section is not modeling the stability of Ti phases accurately. The garnet-subtracted XRF-derived composition section shown in Figure 7a shows the predicted P–T stability of the peak assemblage observed in the sample (Grt + Ms +Bt + Pl + Ky + Qtz + Ilm). Comparison of Figure 6a and 7a indicates that the upper-pressure stability limit of this assemblage is decreased a minor amount owing to changes in effective bulk-rock composition induced by garnet growth. Multi-equilibria garnet-rim thermobarometry (method described in Powell & Holland 1994) was applied to this sample using garnet-edge and matrix-phase compositions (Table 1) and the program THERMOCALC in Average-PT mode. The resulting P–T condition is 7.2 (±0.7) kilobars and 680 (±47)°C, with uncertainty at the 1σ level. We consider the overlap of the uncertainty ellipse generated by garnet-rim thermobarometry with the field of the peak mineral-assemblage to represent the best estimate of garnet-rim (interpreted as peak) metamorphic P–T conditions. This field is shown in red on Figure 7b. There is no statistically significant difference in pressure between growth conditions for the core and rim, suggesting an isobaric heating path during garnet growth. Technically, this represents a garnet-growth vector, and not a P–T path. However, we see no evidence in the chemical zoning in garnet to suggest any significant changes in pressure during garnet growth, and therefore believe that an isobaric heating path is the best interpretation for garnet growth in this case.

Discussion and Conclusions

Isochemical P–T phase-diagram sections provide important information on mineral-assemblage stability in P–T space. There are three main factors that lead to uncertainty in the application of these diagrams to natural samples, namely uncertainty in thermodynamic data, uncertainty in activity–composition relationships, and uncertainty in effective bulk-compositions. The uncertainty in effective bulk-composition is quite problematic, and probably the most overlooked in recent studies. It is clear that the effective bulk-composition for a sample changes with growth of zoned phases and with a change in composition of the infiltrating fluid. Perhaps one of the largest changes in effective composition occurs during the process of partial melting, where the melt is effectively removed from the remaining residue (White & Powell 2002). This change in composition during partial melting commonly is neglected because there is no definitive way to determine exactly how much melt has been removed from the sample, and just when, in the reaction history of the residue, this melt was removed. However, changes in bulk-rock composition due to growth of zoned phases can at least be considered in a semiquantitative manner, provided the zoned phases in question are still present, and their chemical zoning is retained. We say that they can be modeled semiquantitatively only, because there is still the uncertainty on how much the rock's composition changed owing to fluid flux during the reaction history.

A further problem in determining the effective bulk-composition involves the uncertainty on how to deal with samples that are compositionally layered at the scale of a thin section. In such a case, it is clear that the effective bulk-composition is not constant across the section, or there would not be any layering. In such cases, quantitative X-ray mapping will be required to isolate individual layers and model the layers on an individual basis. In addition, for samples containing porphyroblasts that are not chemically zoned (such as kyanite for sample MC–01–97), it is not clear if the interiors of these crystal should contribute to the bulk-rock composition available to the reacting assemblage of phases if diffusion of elements through the crystal structure is slow relative to the growth or consumption rate of matrix phases. This problem is currently being investigated.

Two fundamental methods used for determining effective bulk-compositions in samples with chemically zoned phases include X-ray-fluorescence analysis and quantitative X-ray mapping. As discussed above, the technique used should be determined by the goal of the modeling and the nature of the sample. Application of quantitative X-ray mapping to the calculation of changes in effective bulk-composition due to growth of chemically zoned garnet is ideally suited to samples containing small crystals of garnet, such that a sufficient area can be mapped in a reasonable amount of time to obtain a representative composition (see Marmo *et al*. 2002). In this study, the size of the crystals precluded the use of quantitative X-ray mapping for determining a bulk-rock composition appropriate for initial nucleation and growth of garnet. In this case, the best method with

FIG. 5. Maps of oxide (molar proportions) produced from X-ray maps of MC–01–97. (a) Al_2O_3, (b) CaO, (c) FeO, (d) MgO, (e) MnO, (f) MnO with garnet selectively removed. Only the remaining visible garnet pixels in (f) were used to obtain the integrated composition of garnet to remove from the bulk-rock XRF-derived composition. The large grain of garnet is the same as that shown in Figure 2.

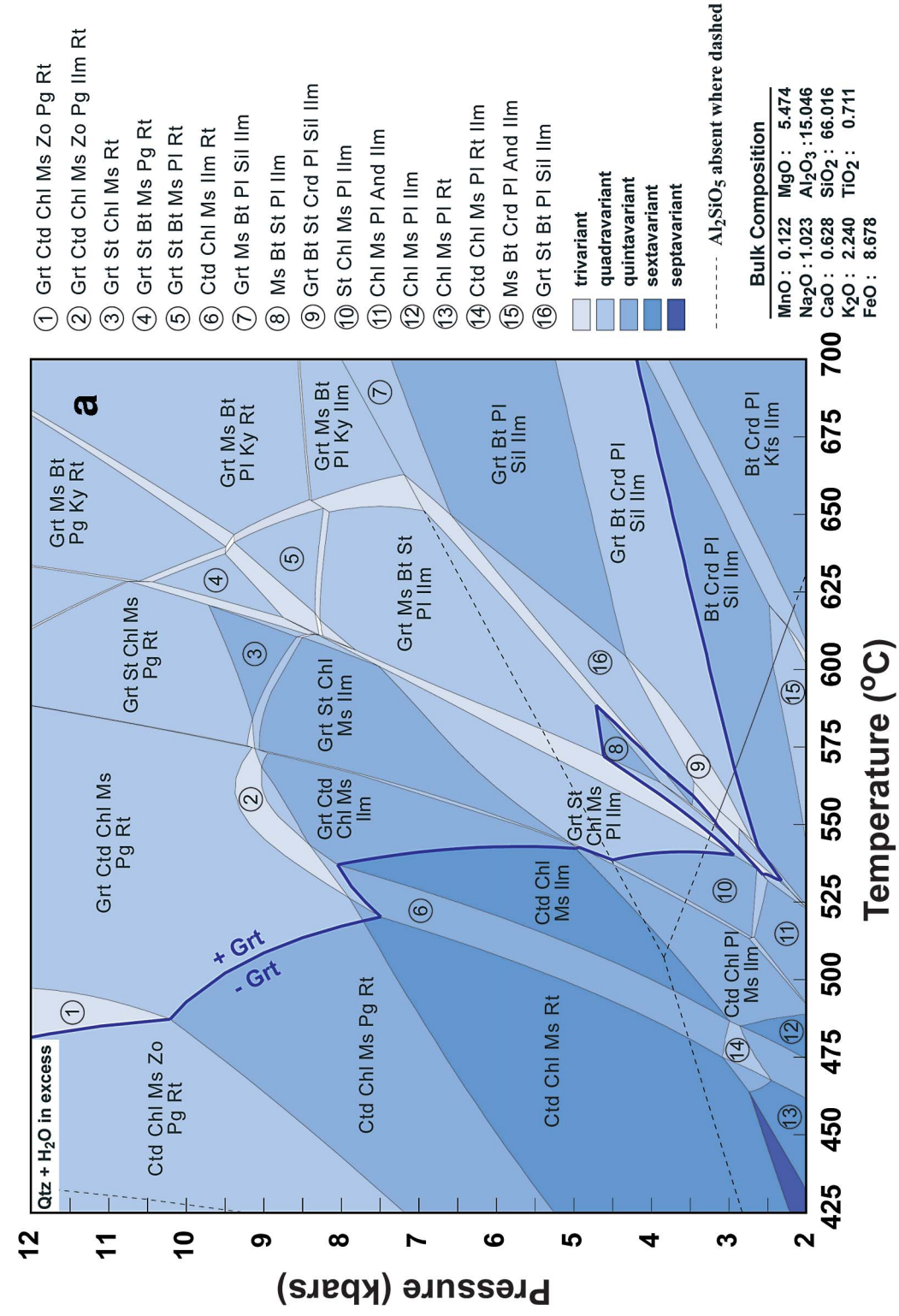
① Grt Ctd Chl Ms Zo Pg Rt
② Grt Ctd Chl Ms Zo Pg Ilm Rt
③ Grt St Chl Ms Rt
④ Grt St Bt Ms Pg Rt
⑤ Grt St Bt Ms Pl Rt
⑥ Ctd Chl Ms Ilm Rt
⑦ Grt Ms Bt Pl Sil Ilm
⑧ Ms Bt St Pl Ilm
⑨ Grt Bt St Crd Pl Sil Ilm
⑩ St Chl Ms Pl Ilm
⑪ Chl Ms Pl And Ilm
⑫ Chl Ms Pl Ilm
⑬ Chl Ms Pl Rt
⑭ Ctd Chl Ms Pl Rt Ilm
⑮ Ms Bt Crd Pl And Ilm
⑯ Grt St Bt Pl Sil Ilm
trivariant
quadravariant
quintavariant
sextavariant
septavariant
Al_2SiO_5 absent where dashed
Bulk Composition
MnO : 0.122 MgO : 5.474
Na_2O : 1.023 Al_2O_3 : 15.046
CaO : 0.628 SiO_2 : 66.016
K_2O : 2.240 TiO_2 : 0.711
FeO : 8.678
a
Qtz + H_2O in excess
Ctd Chl Ms Zo Pg Rt
Grt Ctd Chl Ms Pg Rt
Ctd Chl Ms Pg Rt
Ctd Chl Ms Rt
+ Grt
- Grt
Grt St Chl Ms Pg Rt
Grt Ctd Chl Ms Ilm
Grt St Chl Ms Ilm
Ctd Chl Ms Ilm
Grt St Chl Pl Ilm
Ctd Chl Pl Ms Ilm
Grt Ms Bt Pg Ky Rt
Grt Ms Bt Pl Ky Rt
Grt Ms Bt St Pl Ilm
Grt Ms Bt Pl Ky Ilm
Grt Bt Pl Sil Ilm
Grt Bt Crd Pl Sil Ilm
Bt Crd Pl Sil Ilm
Bt Crd Pl Kfs Ilm
Pressure (kbars)
Temperature (°C)
12
11
10
9
8
7
6
5
4
3
2
425
450
475
500
525
550
575
600
625
650
675
700

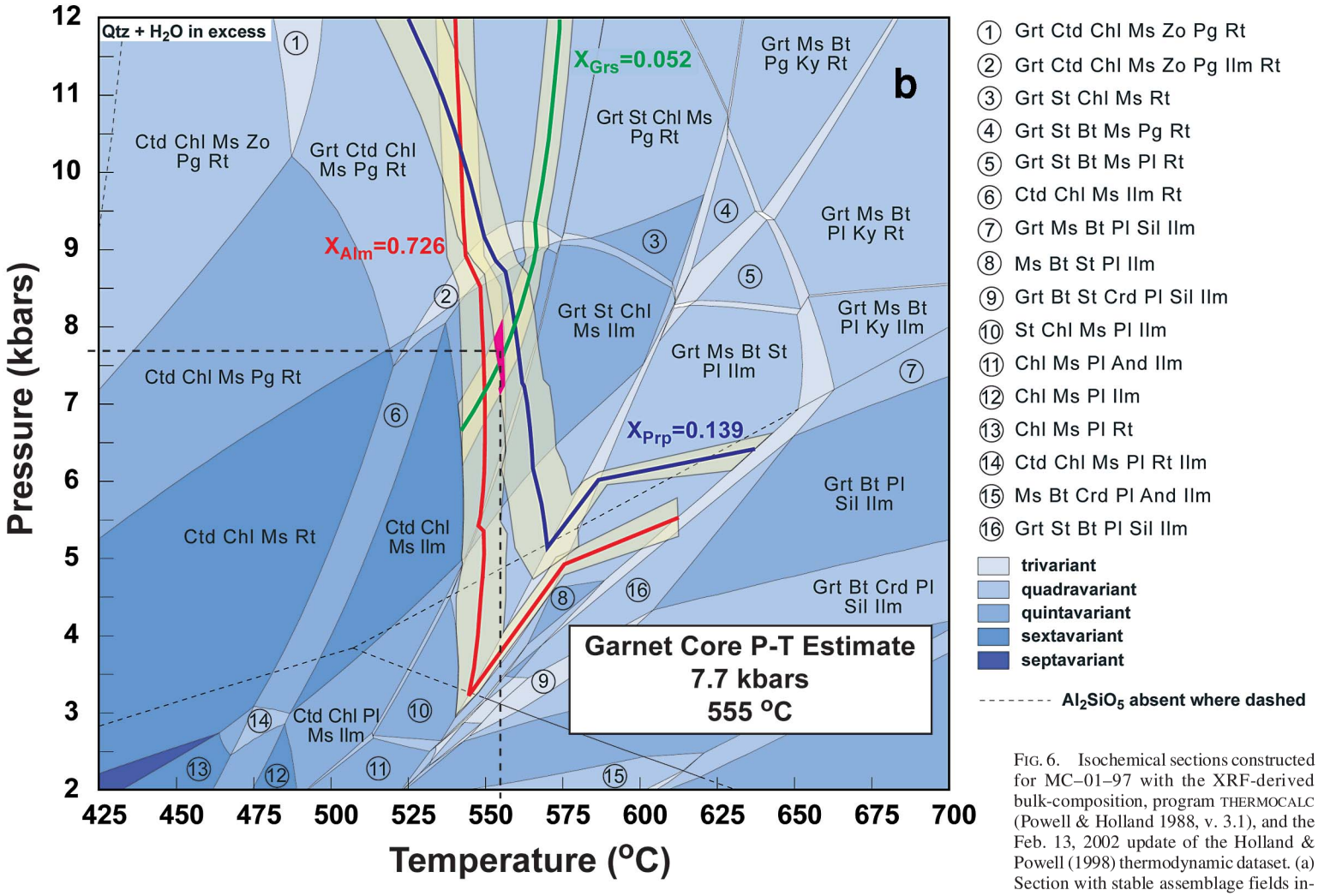

FIG. 6. Isochemical sections constructed for MC–01–97 with the XRF-derived bulk-composition, program THERMOCALC (Powell & Holland 1988, v. 3.1), and the Feb. 13, 2002 update of the Holland & Powell (1998) thermodynamic dataset. (a) Section with stable assemblage fields indicated and bulk composition indicated. Fields colored by assemblage variance. Thick blue line separates the P–T space in which garnet is not stable from that in which garnet is stable. Quartz and H_2O were assumed to be in excess in the calculations. (b) Section with measured isopleths in the garnet core for the independent members almandine (Alm), pyrope (Prp), and grossular (Grs) shown. Uncertainty in location of isopleths (calculated by THERMOCALC) are indicated by yellow bands. The overlap of these uncertainty bands (indicated by red polygon) is taken as the best estimate for P–T conditions of growth of the garnet core (approximately 7.7 kbar, 555°C).

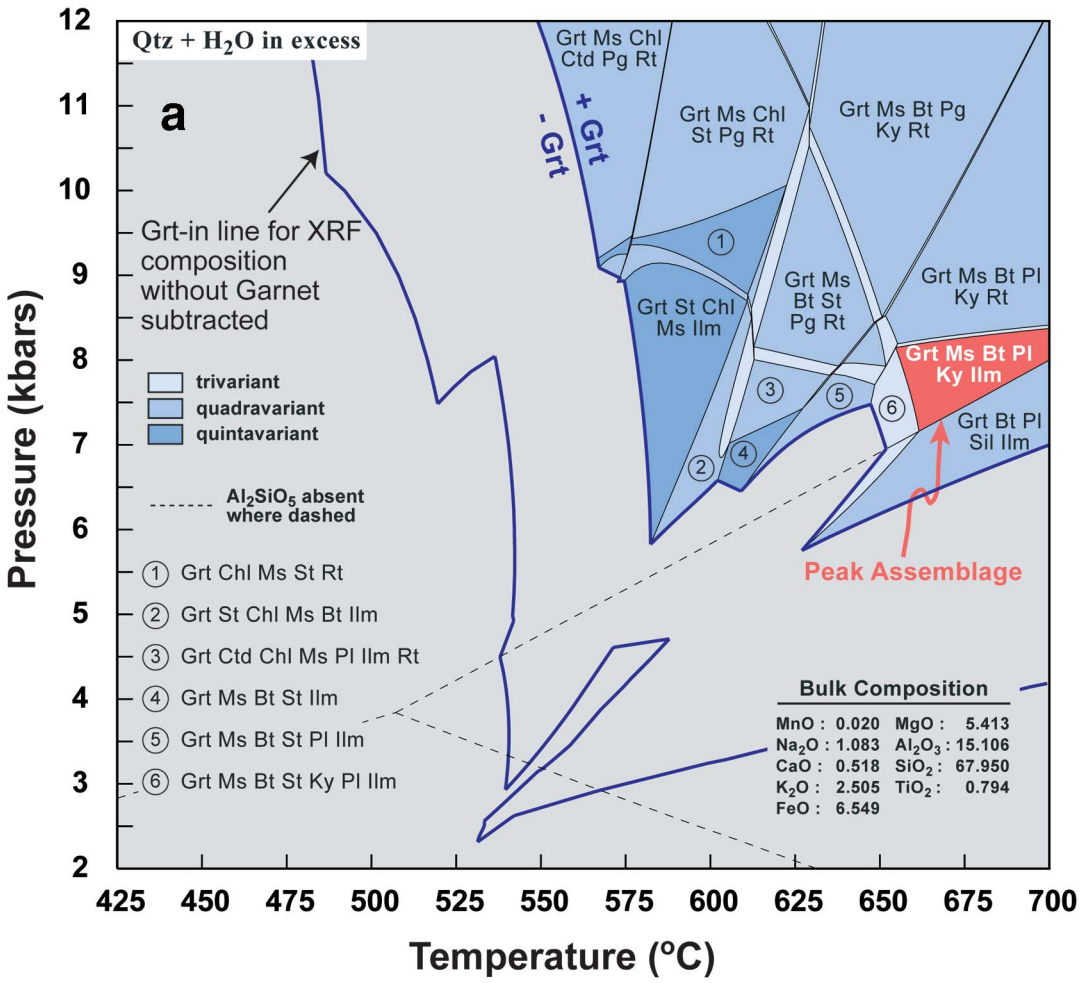

which to obtain a bulk composition appropriate for the modeling of initial growth of garnet is X-ray-fluorescence analysis. However, obtaining a composition appropriate for modeling peak metamorphism required removal of chemically zoned garnet. Quantitative X-ray mapping provided a means to obtain an integrated composition of garnet to subtract from the bulk-rock composition, in order to model peak metamorphism with isochemical sections. There is a potential problem in determining exactly how much garnet should be removed from the bulk-rock composition to model the peak assemblage. Should all of the garnet be removed, or should some of the garnet rim remain in the bulk-rock composition? If one decides that some of the rim material should remain, there are technical problems in processing the maps that would allow one to select the appropriate analytical points on a map to remain in the rock, and a decision would have to be made as to just how much of the rim should remain (a rim 2, 5, or even 100 μm wide?). However, it should be noted that along an assemblage field-boundary, the mode and compositions of phases are contiguous across the assemblage boundary. Therefore, removing all of the garnet from the bulk-rock composition is equivalent to assuming there is an infinitesimally small amount of garnet in equilibrium with the matrix assemblage, and that is the assumption made in this study.

This combined technique allows estimation of P–T conditions of growth of both garnet core and garnet rim, and hence a P–T vector for garnet growth. Using the combined technique, garnet-growth metamorphism at Mica Dam was constrained to occur during an isobaric heating event. The lack of significant chemical zoning in the grossular component of garnet indicates there was no significant pressure change during garnet growth, and we therefore take the derived P–T vector as the best

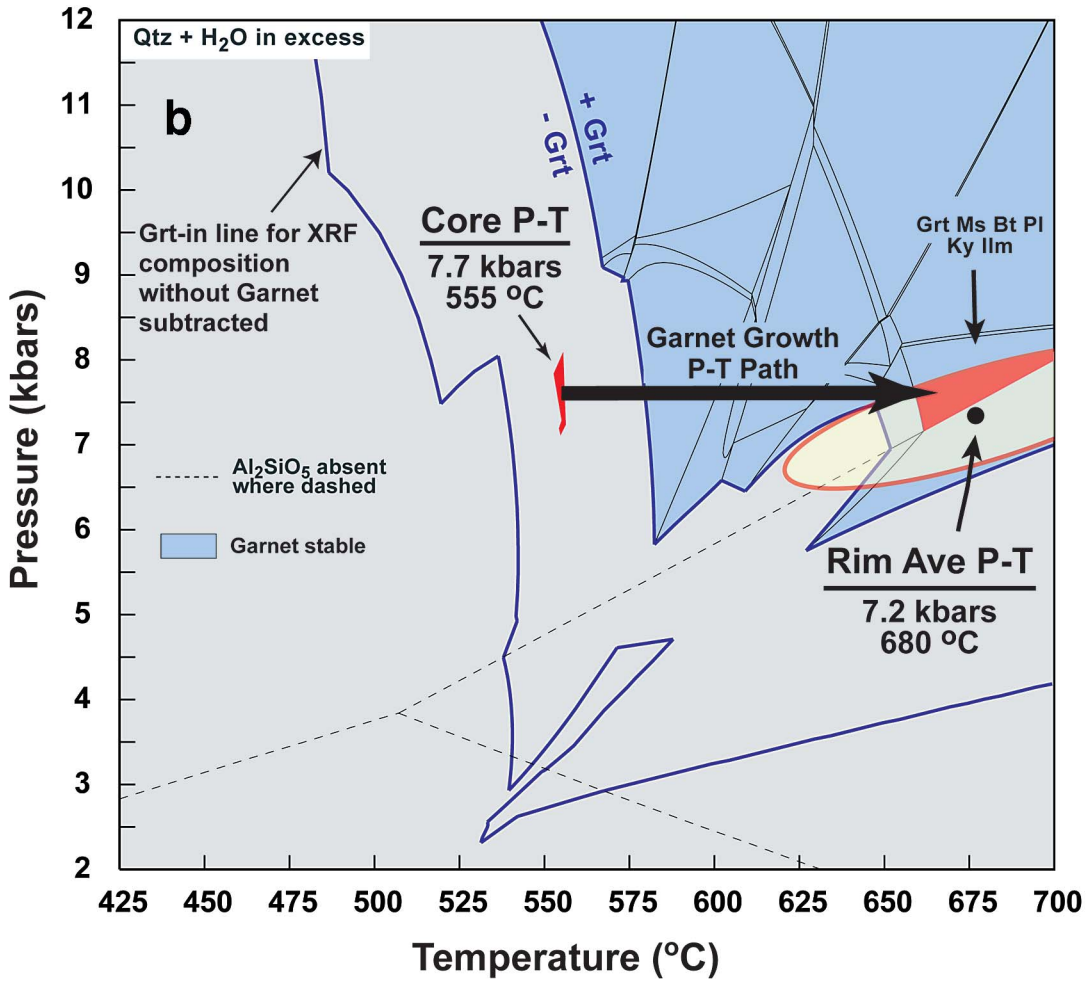

FIG. 7. Isochemical sections constructed for MC–01–97 using the XRF-derived bulk-composition with garnet subtracted, program THERMOCALC (Powell & Holland 1988, v. 3.1), and the Feb. 13, 2002 update of the Holland & Powell (1998) thermodynamic dataset. (a) Section showing only the garnet-stable assemblages and bulk composition. The garnet-in line for the XRF-derived composition used in Figure 6 and the garnet-in line for this bulk composition are shown to indicate the effect of garnet fractionation on garnet stability. The field corresponding to the observed assemblage (interpreted as the peak assemblage) is highlighted in red. (b) Section shown in (a) with the estimated P–T path of garnet growth, shown by large arrow. All garnet-stable fields are shown in a single blue color for simplicity. The result of garnet-rim thermobarometry is indicated, with an uncertainty ellipse (calculated by THERMOCALC) shown in yellow. The overlap of the peak-assemblage field and the uncertainty ellipse is taken as the best estimate for P–T conditions of growth of the garnet rim and is shown in red. The P–T estimate for the garnet core from Figure 6b is indicated by the red polygon centered at 555°C.

estimate for the P–T path followed during garnet-growth metamorphism at Mica Dam.

ACKNOWLEDGEMENTS

This research was funded by an NSERC Discovery grant to E.D. Ghent. We thank F. Brouwer, H. Stowell, and M. St-Onge for providing constructive reviews that led to improvement and clarification of the manuscript. It is a pleasure to contribute this article in celebration of the career of Dugald M. Carmichael, whose work has both influenced our thoughts on metamorphic processes and served as a guide in discovering the P–T histories of metamorphism.

References

BENCE, A.E. & ALBEE, A.E. (1968): Empirical correction factors for the electron microanalysis of silicates and oxides. *J. Geol.* **76**, 382-403.

CLARKE, G.L., DACZKO, N.R. & NOCKOLDS, C. (2001): A method for applying matrix corrections to X-ray intensity maps using the Bence–Albee algorithm and Matlab. *J. Metamorph. Geol.* **19**, 653-644.

COGGON, R. & HOLLAND, T.J.B. (2002): Mixing properties of phengitic micas and revised garnet–phengite thermobarometers. *J. Metamorph. Geol.* **20**, 683-696.

CONNOLLY, J.A.D. & CESARE, B. (1993): C–O–H–S fluid composition and oxygen fugacity in graphitic metapelites. *J. Metamorph. Geol.* **11**, 379-388.

_____ & PETRINI, K. (2002): An automated strategy for calculation of phase diagram sections and retrieval of rock properties as a function of physical conditions. *J. Metamorph. Geol.* **20**, 697-708.

CROWLEY, J.L., GHENT, E.D., CARR, S.D., SIMONY, P.S. & HAMILTON, M.A. (2000): Multiple thermotectonic events in a continuous metamorphic sequence, Mica Creek area, southeastern Canadian Cordillera. *Geol. Mat. Res.* **2**, 1-45.

DIGEL, S.D., GHENT, E.D., CARR, S.D. & SIMONY, P.S. (1998): Early Cretaceous kyanite–sillimanite metamorphism and Paleocene sillimanite overprint near Mt. Cheadle, southeastern British Columbia: geometry, geochronology, and metamorphic implications. *Can. J. Earth. Sci.* **35**, 1070-1087.

GHENT, E.D. & GORDON, T.M. (2000): Application of INVEQ to the geothermobarometry of metamorphic rocks near a kyanite–sillimanite isograd, Mica Creek, British Columbia. *Am. Mineral.* **85**, 9-13.

_____, STOUT, M.Z. & PARRISH, R.R. (1989) Determination of metamorphic pressure–temperature–time (P–T–t) paths. *In* Heat, Metamorphism and Tectonics (E.G. Nisbet & C.M.R. Fowler, eds.). *Mineral. Assoc. Can., Short-Course Vol.* **14**, 155-188.

_____ & VALLEY, J.W. (1998): Oxygen isotope study of quartz–Al_2SiO_5 pairs from the Mica Creek area, British Columbia; implications for the recovery of peak metamorphic temperatures. *J. Metamorph. Geol.* **16**, 223-230.

HOLLAND, T.J.B. & POWELL, R. (1998): An internally consistent thermodynamic data set for phases of petrological interest. *J. Metamorph. Geol.* **16**, 309-343.

KELSEY, D.E., WHITE, R.W. & POWELL, R. (2003): Orthopyroxene – sillimanite – quartz assemblages: distribution, petrology, quantitative P–T–X constraints and P–T paths. *J. Metamorph. Geol.* **21**, 439-453.

KRETZ, R. (1983): Symbols for rock-forming minerals. *Am. Mineral.* **68**, 277-279.

MARMO, B.A., CLARKE, G.L. & POWELL, R. (2002): Fractionation of bulk rock composition due to porphyroblast growth: effects on eclogite facies mineral equilibria, Pam Peninsula, New Caledonia. *J. Metamorph. Geol.* **20**, 151-165.

POWELL, R. & HOLLAND, T.J.B. (1988): An internally consistent dataset with uncertainties and correlations. 3. Applications to geobarometry, worked examples and a computer program. *J. Metamorph. Geol.* **6**, 173-204.

_____ & _____ (1993): On the formulation of simple mixing models for complex phases. *Am. Mineral.* **78**, 1174-1180.

_____ & _____ (1994): Optimal geothermometry and geobarometry. *Am. Mineral.* **79**, 120-133.

_____ & _____ (1999): Relating formulations of the thermodynamics of mineral solid solutions: activity modeling of pyroxenes, amphiboles, and micas. *Am. Mineral.* **84**, 1-14.

RAESIDE, R.P. & SIMONY, P.S. (1983): Stratigraphy and deformational history of the Scrip Nappe, Monashee Mountains, British Columbia. *Can. J. Earth. Sci.* **20**, 639-650.

SPEAR, F.S. (1993): *Metamorphic Phase Equilibria and Pressure – Temperature – Time Paths*. Mineralogical Society of America, Washington D.C.

_____ & SELVERSTONE, J. (1983): Quantitative P–T path from zoned minerals; theory and tectonic applications. *Contrib. Mineral. Petrol.* **83**, 348-357.

ST-ONGE, M.R. (1987): Zoned poikiloblastic garnets: P–T paths and syn-metamorphic uplift through 30 km of structural depth, Wopmay Orogen, Canada. *J. Petrol.* **28**, 1-22.

STOWELL, H.H. & TINKHAM, D.K. (2003): Integration of phase equilibria modelling and garnet Sm–Nd chronology for construction of P–T–t paths: examples from the Cordilleran Coast Plutonic Complex, USA. *In* Geochronology: Linking the Isotopic Record with Petrology and Textures (D. Vance, W. Müller & I. Villa, eds.). *Geol. Soc., Spec. Publ.* **220**, 119-145.

STÜWE, K. (1997): Effective bulk composition changes due to cooling: a model predicting complexities in retrograde reaction textures. *Contrib. Mineral. Petrol.* **129**, 43-52.

TINKHAM, D.K. (2002): *MnNCKFMASH Metapelite Phase Equilibria, Garnet Activity Modeling, and Garnet Samarium–Neodymium Chronology: Applications to the Waterville Formation, Maine, and south-central Nason Terrane, Washington.* Ph.D. thesis, Univ. of Alabama, Tuscaloosa, Alabama.

_____ & GHENT, E.D. (2005): XRMapAnal: a program for analysis of quantitative X-ray maps. *Am. Mineral.* **90** (in press).

_____, ZULUAGA, C.A. & STOWELL, H.H. (2001): Metapelite phase equilibria modeling in MnNCKFMASH: the effect of variable Al_2O_3 and MgO/(MgO + FeO) on mineral stability. *Geol. Mat. Res.* **3**, 1-42.

VANCE, D. & MAHAR, E. (1998): Pressure–temperature paths from P–T pseudosections and zoned garnets: potential, limitations and examples from the Zanskar Himalaya, NW India. *Contrib. Mineral. Petrol.* **132**, 225-245.

WHITE, R.W. & POWELL, R. (2002): Melt loss and the preservation of granulite facies mineral assemblages. *J. Metamorph. Geol.* **20**, 621-623.

_____, _____, HOLLAND, T.J.B. & WORLEY, B.A. (2000): The effect of TiO_2 and Fe_2O_3 on metapelitic assemblages at greenschist and amphibolite facies conditions: mineral equilibria calculations in the system K_2O–FeO–MgO–Al_2O_3–SiO_2–H_2O–TiO_2–Fe_2O_3. *J. Metamorph. Geol.* **18**, 497-511.

Received October 17, 2003, revised manuscript accepted June 24, 2004.

APPENDIX: ACTIVITY–COMPOSITION RELATIONSHIPS

Activity models used for the MnNCKFMASHT phase diagram sections follow those of Tinkham *et al*. (2001), with the following exceptions. The white mica models follow those presented by Coggon & Holland (2002). Muscovite was allowed to mix in the NCKFMASH system, whereas paragonite and margarite mixing was restricted to the system NCKASH. The margarite–paragonite interaction parameter was increased to 24.5 kJ/mol to allow immiscibility at temperatures up to 600°C. Ilmenite was formulated with ideal mixing between the phase components ilmenite, geikielite, and pyrophanite. Non-ideal activity models that differ from those of Tinkham *et al*. (2001) are given below. Phase-component names and abbreviations listed below follow those given in the Holland & Powell (1998) thermodynamic dataset for clarity. Phase-component formulas are given in Holland & Powell (1998) and cited references.

Biotite: K ^{M1}[Fe,Mg,Mn,Al,Ti] ^{M2}[Fe,Mg,Mn,□] ^{T2}[Si,Al] Si_2O_{10} $(OH)_2$

Biotite is modeled in the system MnKFMASHT with the six independent components, phlogopite (Phl), annite (Ann), eastonite (East), Mn-biotite (Mnbi), Ti-biotite (Tibi), and "ordered biotite" (Obi), an octahedrally ordered Fe–Mg component (Powell & Holland 1999, White *et al.* 2000). Mixing of the Tibi component follows the site-occupancy scheme used in White *et al*. (2000). Biotite mixing is described by the following five variables:

$$x_1 = [\mathrm{Fe}/(\mathrm{Fe}+\mathrm{Mg})]^{M1},\ x_2 = [\mathrm{Fe}/(\mathrm{Fe}+\mathrm{Mg})]^{M2},$$
$$y = X^{M1}_{\mathrm{Al}},\ mn = X^{M1}_{\mathrm{Mn}},\ ti = X^{M1}_{\mathrm{Ti}}$$

Site fractions in terms of compositional variables are: $X^{M1}_{\mathrm{Al}} = y$; $X^{M1}_{\mathrm{Fe}} = (1 - y - mn - ti)\ x_1$; $X^{M1}_{\mathrm{Mg}} = (1 - y - mn - ti)\ (1 - x_1)$; $X^{M1}_{\mathrm{Mn}} = mn$; ; $X^{M1}_{\mathrm{Ti}} = ti$; $X^{M2}_{\mathrm{Fe}} = (1 - mn - ti/2)\ x_2$; $X^{M2}_{\mathrm{Mg}} = (1 - mn - ti/2)\ (1 - x_2)$; $X^{M2}_{\mathrm{Mn}} = mn$; $X^{M2}_{\square} = ti/2$; $X^{T1}_{\mathrm{Al}} = (1 - y)\ /\ 2$; $X^{T1}_{\mathrm{Si}} = (1 - y)\ /\ 2$.

The ideal activities of the phase components are expressed as:

$$a^{\mathrm{ideal}}_{\mathrm{Phl}} = 4\ X^{M1}_{\mathrm{Mg}}\ (X^{M2}_{\mathrm{Mg}})^2\ X^{T1}_{\mathrm{Al}}\ X^{T1}_{\mathrm{Si}}$$

$$a^{\mathrm{ideal}}_{\mathrm{Ann}} = 4\ X^{M1}_{\mathrm{Fe}}\ (X^{M2}_{\mathrm{Fe}})^2\ X^{T1}_{\mathrm{Al}}\ X^{T1}_{\mathrm{Si}}$$

$$a^{\mathrm{ideal}}_{\mathrm{East}} = X^{M1}_{\mathrm{Al}}\ (X^{M2}_{\mathrm{Mg}})^2\ (X^{T1}_{\mathrm{Al}})^2$$

$$a^{\mathrm{ideal}}_{\mathrm{Obi}} = 4\ X^{M1}_{\mathrm{Fe}}\ (X^{M2}_{\mathrm{Mg}})^2\ X^{T1}_{\mathrm{Al}}\ X^{T1}_{\mathrm{Si}}$$

$$a^{\mathrm{ideal}}_{\mathrm{Mnbi}} = 4\ X^{M1}_{\mathrm{Mn}}\ (X^{M2}_{\mathrm{Mn}})^2\ X^{T1}_{\mathrm{Al}}\ X^{T1}_{\mathrm{Si}}$$

$$a^{\mathrm{ideal}}_{\mathrm{Tibi}} = 16\ X^{M1}_{\mathrm{Ti}}\ (X^{M2}_{\square})^2\ X^{M2}_{\mathrm{Mg}}\ X^{T1}_{\mathrm{Al}}\ X^{T1}_{\mathrm{Si}}$$

The proportions of each component in the biotite phase are defined as:

$$\mathrm{P}_{\mathrm{Phl}} = (1 - x_1)\ (1 - y - mn - ti)$$

$$\mathrm{P}_{\mathrm{Ann}} = (x_2)\ (1 - mn - ti\ /\ 2)$$

$$\mathrm{P}_{\mathrm{East}} = y$$

$$\mathrm{P}_{\mathrm{Obi}} = (1 - y - mn - ti)\ x_1 - (1 - mn - ti\ /\ 2)\ x_2$$

$$\mathrm{P}_{\mathrm{Mnbi}} = mn$$

$$\mathrm{P}_{\mathrm{Tibi}} = ti$$

Non-ideality is expressed using symmetric formalism (Powell & Holland 1993), with interaction parameters from Powell & Holland (1999) for KFMASH biotite and the Tibi interaction parameters of White *et al*. (2000). All Mnbi parameters are set to zero. The interaction parameters, in kJ/mol end-member, are: $W_{\mathrm{Phl-Ann}} = 9$; $W_{\mathrm{Phl-East}} = 10$; $W_{\mathrm{Phl-Obi}} = 3$; $W_{\mathrm{Ann-East}} = -1$; $W_{\mathrm{Ann-Obi}} = 6$; $W_{\mathrm{East-Obi}} = 10$; $W_{\mathrm{Phl-Tibi}} = -10$; $W_{\mathrm{Ann-Tibi}} = 12$; $W_{\mathrm{Obi-Tibi}} = 0$; $W_{\mathrm{East-Tibi}} = 0$.

Staurolite: $[Fe,Mg,Mn]_4\ Al_{18}\ Si_{7.5}\ O_{48}\ H_4$

Staurolite is modeled in MnFMASH with the three independent components, Fe-staurolite (Fst), Mg-Staurolite (Mst), and Mn-Staurolite (Mnst). Activities are expressed as: $a_{Mst} = X^4_{Mg}$; $a_{Fst} = X^4_{Fe}$, and $a_{Mnst} = X^4_{Mn}$. Non-ideal mixing was considered between the Fe and Mg phase-components, with the interaction parameter $W_{Fst-Mst} = -8$ kJ/mol.

Chloritoid: $[Fe,Mg,Mn]\ Al_2\ SiO_5\ (OH)_2$

Chloritoid is modeled in MnFMASH with the three independent phase-components Mg-chloritoid (Mctd), Fe-chloritoid (Fctd), and Mn-Chloritoid (Mnctd). Activities are expressed as: $a_{Mctd} = X_{Mg}$; $a_{Fctd} = X_{Fe}$, and $a_{Mnctd} = X_{Mn}$. Non-ideal mixing was considered between the Fe and Mg components, with the interaction parameter $W_{Mtcd-Fctd} = 1$ kJ/mol (Holland & Powell 1998).